On the signatures of oxygen vacancies in O1s core level shifts

Surface Science 705 (2021) 121761

Contents lists available at ScienceDirect

Surface Science

journal homepage: www.elsevier.com/locate/susc

On the signatures of oxygen vacancies in O1s core level shifts

Alvaro Posada-Borbón, Noemi Bosio, Henrik Grönbeck *

Competence Centre for Catalysis and Department of Physics, Chalmers University of Technology, Göteborg, SE-412 96 Sweden

ARTICLE INFO

Keywords:
Core Level Shifts
DFT
Oxides

ABSTRACT

Density functional theory calculations are used to investigate O1s surface core level shifts for MgO(100), ZnO $(10\bar{1}0)$, $In_2O_3(111)$ and $CeO_2(111)$. Shifts are calculated for the pristine surfaces together with surfaces containing oxygen vacancies and dissociated H_2. Pristine surfaces show small negative shifts with respect to the bulk components and vacancies are found to have a minor effect on the O1s binding energies of neighboring oxygen atoms. OH-groups formed by H_2 dissociation yield binding energies shifted to higher energies as compared to the oxygen atoms in the bulk. The results stress the difficulties in assigning core-level shifts and suggest that assignments of shifts in O1s binding energies to neighboring oxygen vacancies for the explored oxides should be reconsidered.

1. Introduction

X-ray photoemission spectroscopy (XPS) is a common technique for chemical analysis [1]. By use of synchrotron radiation, it is possible to obtain an energy resolution that enable separation between electronic binding energies that originate from surface and bulk atoms [2]. The high sensitivity of core level shifts (CLS) to the character of the bond and local structure, gives in many cases unique signatures. Thanks to the high sensitivity, measurements of surface CLS have become a complementary technique to unravel, for example, reconstructions of metal surfaces upon molecular adsorption [3] or strain-patterns [4].

The measured CLS reflects both the chemical state of the considered atom and the possibility of the valence electrons to screen the core-hole that is created in the photoemission process. The differences in screening gives rise, for example, to different signs of the surface CLS of metals to the left and right in the period table of elements [5]. Metals to the left have a positive shift, whereas metals to the right have a negative shift. The positive (negative) shift arises as the screening occurs in states with bonding (antibonding) character. Moreover, it is crucial whether the screening takes place in d- or s-derived states as the screening is more efficient in states with d-character. One striking consequence of the character of the state that screens the core-hole is the opposite signs of the 3d surface CLS of Pd and Ag upon oxidation [6].

Because of the complexity in the origin of electronic binding energies, first principles calculations are often used to assist the interpretation of measured CLS. Such combined experimental and computational efforts have in the past focussed mainly on metallic surfaces. The studies of well-defined oxide surfaces have been hampered by experimental challenges such as the preparation of defect-free surfaces and charging during the experiments. As many of the challenges have been solved, there is a growing literature on XPS-studies of oxide surfaces.

XPS-analysis of oxide surfaces generally include measurements of the O1s binding. Interestingly, O1s binding energies at higher binding energies than the bulk is commonly assigned to oxygen vacancies in the surface. Such assignments have, for example, been done for ZnO [7–9], and In_2O_3 [10,11]. The binding energy of the O1s state of a bulk atom is given by the energy difference between the pristine system and the system with a core hole for an oxygen atom in the bulk. A positive shift of surface atoms corresponds to a final state that is less stable than when the excitation is done in the bulk. A negative shift corresponds instead to the case when the final state is more stable than when the excitation is done in the bulk. The rational for assigning a positive CLS to neighboring oxygen vacancies is a change in the oxidation state of the cations. In an electrostatic model [12–14], however, the lower cation charge results in a decrease of the Coulomb potential and, therefore, an energetic destabilization of neighboring oxygen anions. Thus, an electrostatic initial state picture does not support the interpretation of positive CLS to the presence of oxygen vacancies. It is clear that the CLS depend sensitively on the electronic screening [2,6,15,16], which makes the situation complicated to analyze.

In the present study, we use DFT calculations to investigate O1s surface core level shifts on MgO(100), ZnO$(10\bar{1}0)$, $In_2O_3(111)$ and

* Corresponding author.
E-mail address: ghj@chalmers.se (H. Grönbeck).

https://doi.org/10.1016/j.susc.2020.121761
Received 16 July 2020; Received in revised form 20 October 2020; Accepted 8 November 2020
Available online 13 November 2020

$CeO_2(111)$ focussing on the effect of neighboring oxygen vacancies. We find for all studied surfaces that oxygen vacancies only slightly change the O1s binding energy of neighboring oxygen atoms. Instead we suggest that the experimental assignments of oxygen vacancies could be related to adsorbates, such as OH-groups.

2. Computational Methods and Modeled Systems

The density functional theory calculations are performed using the Vienna Ab-initio Simulation Package (VASP) [17–20]. The interaction between the valence electrons and the cores is described with the plane augmented wave (PAW) method [21,22]. The valence configurations are $1s^1$ (H), $2s^22p^4$ (O), $2p^63s^2$ (Mg), $3d^{10}4s^2$ (Zn), $4d^{10}5s^25p^1$ (In), and $5s^25p^65d^14f^16s^2$ (Ce). The exchange-correlation effects are described within the generalized gradient approximation according to Perdew, Burke and Ernzerhof (PBE) [23]. Hubbard-U corrections are applied to describe the localization of the 3d (4f) states of Zn (Ce) [24]. Following the literature, a value of 7.5 eV is used for Zn,[25] and 4.5 eV for Ce [26]. The Kohn-Sham orbitals are expanded with plane waves using a 500 eV cut-off.

Structures are optimized with the conjugate gradient method and geometries are considered to be converged when the largest force is smaller than 3×10^{-2} eV/Å. The integration over the Brillouin zone is approximated by finite sampling using a Monkhorst-Pack scheme.[27,28] The considered surfaces are MgO(100), ZnO($10\bar{1}0$), $In_2O_3(111)$ and $CeO_2(111)$ with the corresponding surface cells (3×3), (3×2), (1×1) and ($5 \times 2\sqrt{3}$). The k-point sampling is $2 \times 2 \times 1$ for ZnO($10\bar{1}0$), $3 \times 3 \times 1$ for $In_2O_3(111)$, whereas MgO(100) and $CeO_2(111)$ are treated in the Gamma-point approximation. Surfaces are described by slabs having 7, 9, 5, and 5 layers for MgO(100), ZnO($10\bar{1}0$), $In_2O_3(111)$ and $CeO_2(111)$, respectively. For $In_2O_3(111)$ and $CeO_2(111)$, each layer consists of anion-cation-anion trilayers. The slabs are in all cases separated by at least 15 Å of vaccum.

The core level shifts are calculated assuming complete screening of the core hole. In this method, the CLS is calculated as the total energy difference having the core hole either in the surface or in the center of the slab. The complete screening approach assumes i) that the lifetime of the core hole is long with respect to the photo-emission process, ii) that the system is in the ground state with the constraint of a core hole, and iii) that structural relaxations are negligible. The systems with a core hole are obtained by generating a PAW potential with an electron hole in 1s shell of O [29]. In addition to this ΔE_{tot} method, we also explored the Z+1 approach [30], which is a chemical intuitive method viewing the shift as differences in the chemical stability of the core-excited atom. As the core hole is created close to the nucleus, the environment effectively recognizes a Z+1 atom.

The measured shifts include the final state effects. However, to understand the origin of the shifts it is interesting to analyze initial state effects. Thus, the O1s binding energy before the core excitation. We have done this by calculating the shifts in the O1s Kohn-Sham eigenvalues.

As the periodic boundary conditions exclude the use of charged supercells, charge neutrality needs to be maintained in the presence of a core hole. This can be done either by adding an extra electron to the valence or by use of a compensating charge in the form of a homogeneous jellium background. Adding an extra electron should not be done for systems with band-gaps, as the electron in this case is added in the conduction band. These are states that are not occupied in the experimental situation and have different screening properties than the states in the valence band [31]. As the considered systems have band gaps, we are using charged cells and a compensating jellium background. The approach was evaluated for the, so-called, ESCA molecule (ethyl trifluoroacetate) in Ref. [32].

3. Results and Discussion

The structures of the investigated surfaces are shown in Figure 1. The oxygen atoms are in bulk MgO occupying octahedral positions with six cation neighbors. The number of neighbors on the MgO(100) surface is instead five. The structural relaxation of the surface gives a slight positive rumpling[33], which indicates that the inward relaxation of the anions are smaller than the cations. The oxygen anions are occupying tetrahedral positions in ZnO with four nearest neighbors. The ZnO($10\bar{1}0$) is corrugated where the surface layer consists of two types of oxygen anions. The top-most oxygen atom is under-coordinated, having three cation neighbors. The second oxygen atom has full coordination with four neighbors. Oxygen is four-fold coordinated also in bulk In_2O_3. The $In_2O_3(111)$ surface is heterogeneous and consists of corrugated tri-layers with 16 In atoms. The oxygen atoms located above and below the indium layer are coordinated either in three-fold or four-fold fashions. The oxygen atoms are four-fold coordinated in bulk CeO_2. The $CeO_2(111)$ surface slab consists of tri-layer and the top-most oxygen layer have three-fold coordinated oxygen atoms. All studied surface have a band gap. The calculated gaps are 3.2 eV, 1.5 eV, 0.16 eV, 2.2 eV for MgO(100), ZnO($10\bar{1}0$), $In_2O_3(111)$ and $CeO_2(111)$, respectively. The gaps are smaller than the measured gaps, which, is expected given the applied semi-local exchange correlation functional.

The calculated CLS (ΔE_{tot}) for the bare surfaces are collected in Table 1 and shown in Figure 1. The shift for oxygen atoms in the surface for MgO(100) is slightly negative. This is in agreement with previous reports [34,35]. A small shift is consistent with experiments, where a peak corresponding to the surface cannot be resolved [35].

The two oxygen atoms at the surface of ZnO($10\bar{1}0$) have distinctly different shifts. The three-fold coordinated atom has a negative shift, whereas the four-fold coordinated atom is shifted to higher binding energies. The existence of one negative and one positive component can explain the absence of any measured surface shift for ZnO surfaces [36]. The negative shift for the under-coordinated surface atom is in agreement with a previous report where the four-fold coordinated atom was not considered [37].

For $In_2O_3(111)$, the average O1s CLS for the three-fold [four-fold] O-sites is -0.35 [-0.09] eV, with respect to the O-bulk reference. Among the three-fold coordinated O-sites, the most negative O1s CLS is of -0.79 eV, whereas the rest of three-fold O-sites have small negative shifts. For the four-fold coordinated O-sites, one atom exhibits a slight positive CLS of 0.19 eV, whereas the rest of the atoms have an average CLS of -0.19 eV. The overall energy spread on the calculated CLS suggests one broad feature centered at the binding energy of the bulk atom. The shift for oxygen atoms in the surface of CeO_2 is shifted by -0.48 eV with respect to the bulk component.

The results for the complete CLS (ΔE_{tot}) is in Table 1 compared to the shift of the O1s Kohn-Sham eigenvalue and shifts computed with the Z+1 approach. The eigenvalue analysis gives an impression of the initial state effects, thus the stability of binding energy of the O1s state prior to the emission of the photo-electron. Comparing the shift in eigenvalues and the complete shift shows that the effect of electronic screening is to stabilize the core-hole at the surface with respect to the core hole in the bulk. This is understandable given the larger electronic flexibility at the surface. The largest effect of screening is predicted for CeO_2.

As the investigated surfaces are ionic, the screening is to a large extent located at the site where the core hole is created. A Bader analysis [38,39] reveals that the charge on the anions in the MgO(100) surface is 7.72 electrons for the pristine surface. The charge on an anion with a core hole is calculated to be 7.98 electrons. Thus, the creation of the core-hole attracts only 0.26 electrons and the screening configuration is close to $2p^6$. For ZnO($10\bar{1}0$), the Bader charge on the surface oxygen atoms are 7.24 for the three-fold coordinated anions and 7.29 electrons for the four-fold coordinated anions. In the presence of a core-hole, the corresponding charges are 7.75 and 7.80 electrons, respectively. In this

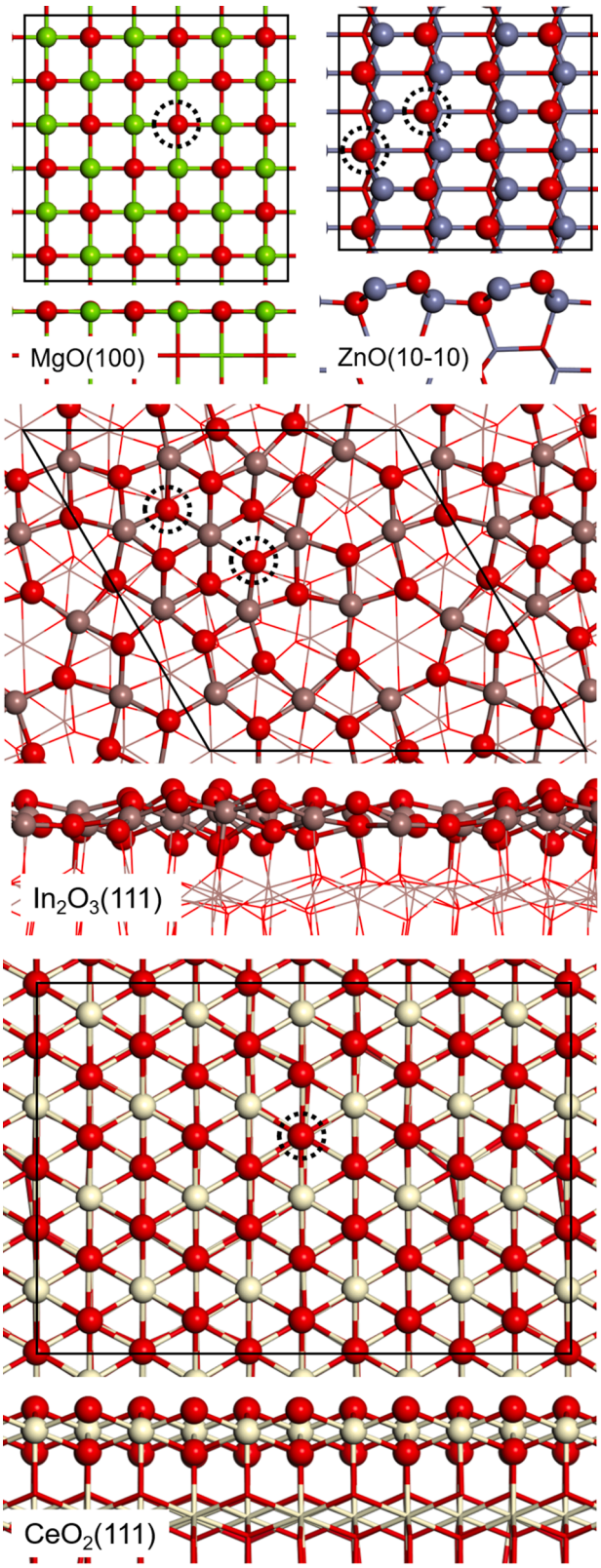

Fig. 1. Top and side views of the investigated surfaces. The surface cells are shown by black lines. The oxygen atoms, which are removed when considering oxygen vacancies are indicated by circles in the top view. Atomic color code: Oxygen (red), magnesium (green), zinc (blue), indium (grey) and cerium (white).

case, the core-hole attracts about 0.5 electrons. For In_2O_3(111), the Bader charge of the three-fold [four-fold] surface oxygen is calculated to be 7.14 [7.20] electrons. The charge changes when the core hole is created to 7.75 and 7.80 for the three- and four-fold atoms, respectively. For CeO_2, the Bader charge on the surface atoms is 7.19 electrons for the pristine surface, whereas the charge in presence of a core-hole is calculated to be 7.80 electrons. Thus, the core-hole attracts in this case about 0.61 electrons. The larger screening charge for ZnO, In_2O_3 and CeO_2 as compared to MgO is connected to the fact that MgO is more ionic than are the other investigated oxides. We note that the final electronic screening configuration is close to $2p^6$ for all investigated oxides.

The CLS with the chemical intuitive Z+1 approach is close to the complete core level shifts. This shows that the core level shifts can be viewed as differences in the stability of an F^- impurity in the oxides. A negative surface shift indicates that it is energetically favorable to have the impurity at the surface.

Turning to the effect of surface oxygen vacancies on the neighboring O1s CLS, we have considered vacancies located in the surface region, see Figure 1. A surface vacancy is for MgO(100) found to be preferred by 0.52 eV as compared to having the vacancy in the sub-surface layer. For ZnO(10$\bar{1}$0), a vacancy in the three-fold position is preferred by 0.46 eV as compared to having the vacancy in the four-fold position. For In_2O_3(111), a surface vacancy in the three-fold position is preferred by 0.31 eV with respect to having a vacancy being in the four-fold configuration. In agreement with previous reports [40,41], we find that the case with a sub-surface vacancy is preferred with respect to the surface vacancy for CeO_2(111) by 0.24 eV.

The effect of oxygen vacancies on the neighboring O1s CLS are reported in Figure 2. The presence of vacancies is found to have a moderate influence on the O1s core level shifts. For MgO(100), oxygen atoms close to the vacancy have a negative shift of -0.36 eV, thus slightly more negative than the unaffected atoms. Creating an oxygen vacancy in the top-most oxygen layer for ZnO(10$\bar{1}$0) has close to no effect on the O1s shifts. Creating instead the vacancy in the four-fold position yields slight negative shifts of about 0.2 eV for both components. For In_2O_3(111), an oxygen vacancy on the three-fold position has a small effect on the surrounding oxygen. The three-fold oxygen sites close to the vacancy have shifts of -0.37 eV, whereas the four-fold O-sites have positive shifts of 0.16 eV. Over the entire slab, the average calculated O1s CLS for the three-fold [four-fold] O-sites is -0.19 [0.09] eV. For CeO_2(111), we calculate the CLS for an oxygen atom close to the vacancy to be -0.44 eV, which is close to the value of the pristine surface.

Analysis of the initial state effects for the cases with vacancies provides a picture that is similar to the pristine surfaces. The initial state shifts as evaluated from the shift in O1s Kohn-Sham eigenvalue are shifted to higher energies again showing that the screening is more efficient on the surface than in the bulk.

The underlying reason for the absence of large shifts of neighboring oxygen atoms in the presence of oxygen vacancies is for MgO and ZnO that the charge density is only slightly changing upon the formation of vacancies. Figure 3 shows the vacancy-induced states in the band gap for

Table 1
O1s surface CLS (in eV) for the considered pristine surfaces calculated with three approximations. $\Delta\epsilon$ is the shift in the O1s Kohn-Sham eigenvalue, ΔE_{tot} is the total energy difference and $Z+1$ is the approximation where energy differences are evaluated with an F impurity.

	$\Delta\epsilon$	ΔE_{tot}	$Z+1$
MgO(100)	0.10	-0.14	-0.13
ZnO(10-10) (3f)	-0.36	-0.47	-0.46
ZnO(10-10) (4f)	0.81	0.60	0.57
In_2O_3(111) (3f)	-0.26	-0.35	-0.31
In_2O_3(111) (4f)	-0.02	-0.09	-0.08
CeO_2(111)	0.39	-0.48	-0.49

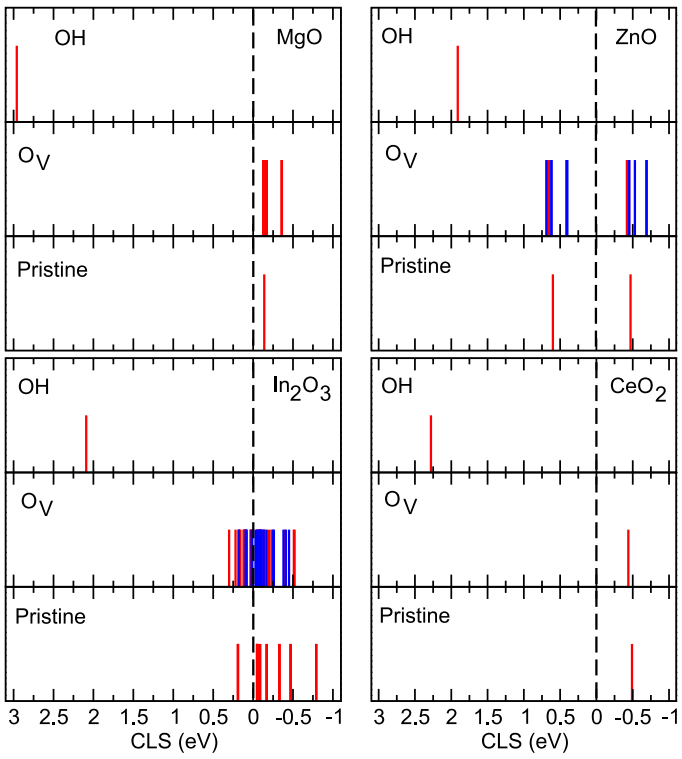

Fig. 2. Core level shifts for MgO(100), ZnO(10$\bar{1}$0), In_2O_3(111) and CeO_2(111). The shifts are calculated with respect to an oxygen atom in the center of the slabs. Pristine, O_V and OH refer to the pristine surface, the surface in presence of an oxygen vacancy and an OH-group formed by H_2 dissociation. For ZnO (10$\bar{1}$0) and In_2O_3, the red (blue) lines correspond to an oxygen vacancy on three-fold (four-fold) position.

MgO(100) and ZnO(10$\bar{1}$0). The density of the vacancy induced state is in both cases stabilized by the Madelung potential and located at the vacancy site. Thus, the charge distribution is not markedly changed as compared to the pristine surface. Moreover, as the screening configuration is $2p^6$, there is only a small amount of charge depleted from the other oxygen anions in the system. The Bader charges on the neighboring oxygen anions having the negative shift on MgO(100), are 7.75 electrons, whereas the charges on the other atoms are unaffected with respect to the pristine surface. The Bader charges for ZnO(10$\bar{1}$0) are unchanged within 0.03 electrons with respect to the pristine surface. The slight negative O1s shift of neighboring oxygen atoms in the presence of a vacancy can be attributed to the fact that the charge at the vacancy site spills out and is not as localized as when attracted to a nuclear charge. The character of the gap-state is for In_2O_3(111) very different. The covalent character of this oxide is manifested by weight on both cation and anion sites.

The situation is again different for CeO_2(111) as ceria is reducible and adopts a formal Ce^{3+} oxidation state upon vacancy formation. The states in the band-gap for CeO_2(111) are localized on two Ce-ions by occupying 4f-states. The charges are localized on Ce-ions that are next-nearest neighbors to the vacancy. However, the vacancy induced shift is also in this case negative as the stabilization of the neighbors is reduced then the cations change from Ce^{4+} to Ce^{3+}. The three oxygen atoms close to the vacancy have a slightly higher charge than in the pristine surface (7.25 electrons). The change in oxidation state of two cerium atoms is evidenced by an increase in the Ce Bader charge from 9.60 for the pristine surface to 9.85 electrons in the presence of a vacancy.

As oxygen vacancies does not result in marked positive shifts in the O1s CLS, we speculate that besides structural changes, other species may result in such shifts. OH-groups are obvious candidates. Dissociated water my result in adsorbed OH-groups and also hydrogen bonded to lattice oxygen sites. We have here investigated the O1s CLS for OH with oxygen being a lattice oxygen. On MgO(100) and ZnO(10$\bar{1}$0) this was

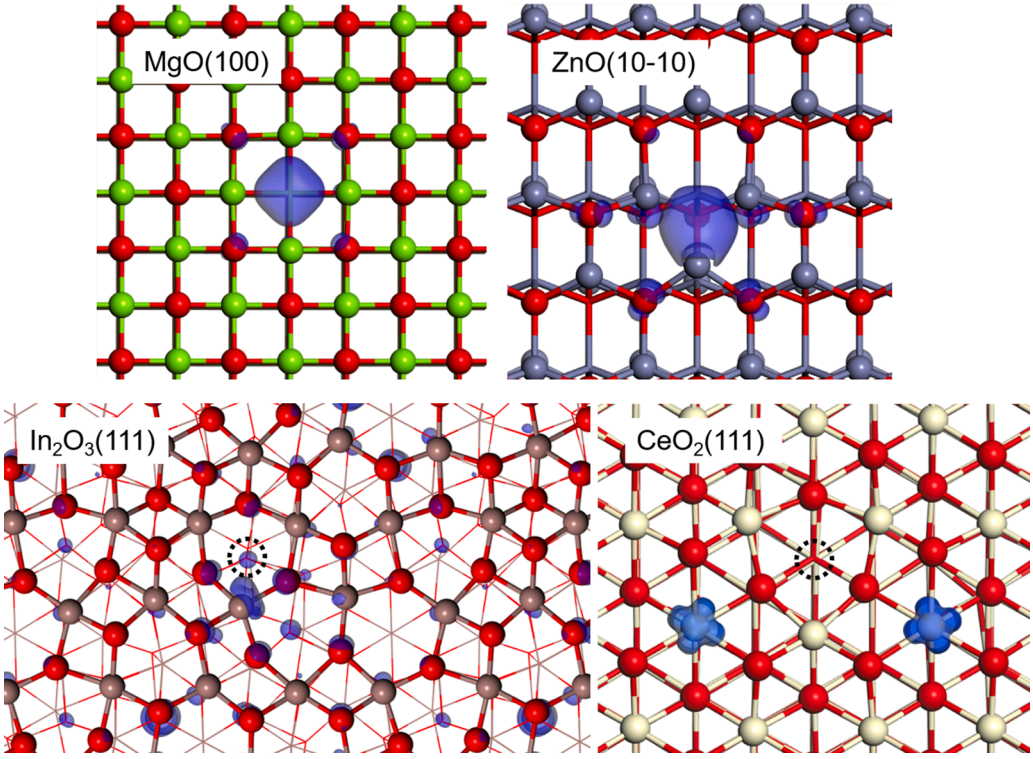

Fig. 3. The charge density of the vacancy induced state in the band-gap. The oxygen atoms, which are removed when considering oxygen vacancies are indicated by circles for In_2O_3(111) and CeO_2(111). The iso-surface of the density is 0.05 e/Å^3 except for In_2O_3(111) where it is 0.01 e/Å^3. The electronic state for the vacancy in CeO_2(111) is a triplet, thus two states are occupied in the band-gap. For simplicity, the iso-surfaces of both states are shown in the figure.

investigated by considering a configuration with H_2 dissociated in an heterolytic fashion, whereas homolytic dissociation has been explored for In_2O_3(111) [42,43] and CeO_2(111) [44].

The O1s CLS for the oxygen atom forming the OH group is calculated to be 2.96 eV for MgO(100), thus clearly separated from the binding energy of the bulk atom. The shift for the OH group on ZnO(10$\bar{1}$0) is calculated to be 1.91 eV.

Homolytic adsorption of H_2 on In_2O_3 surfaces is known to be thermodynamically preferred over the heterolytic case [43]. We consider both cases, and obtain CLS of 1.55 and 2.09 eV for the heterolytic and homolytic adsorption mode, respectively. The difference in O1s CLS between the two modes suggests a difference in nature of the created OH-groups upon hydrogen adsorption. For the heterolytic case, the In-O distance between the hydrated In and O atom changes from 2.14 Å to 2.50 Å upon hydrogen adsorption. For the homolytic case, the largest change in interatomic distance is less pronounced, changing from 2.19 Å on the pristine surface to 2.49 Å upon hydroxylation. The increase in the interatomic distance can be understood as a change in coordination of the OH group formed in the heterolytic adsorption case, which explains the difference in O1s CLS between the two adsorption modes. H_2 dissociates homolytically over CeO_2(111) forming two OH groups [44]. The presence of the two OH-groups is accompanied by the reduction of two cerium cations to Ce^{3+}. The CLS is in this case calculated to be 2.28 eV.

The presence of a proton on the oxygen site results in all cases in large positive shifts, see Figure 2. These shifts could be modified by the presence of other OH-groups and hydrogen bonds [34]. It is not the scope of the present study to explore different configurations of OH-groups on the oxide surface. Here, we merely stress that presence of hydrogen gives rise to CLS that may explain experimental observations that have been assigned to oxygen vacancies.

4. Conclusions

We have investigated the O1s core level shift for MgO(100), ZnO (10$\bar{1}$0), In_2O_3(111) and CeO_2(111). CeO_2(111) is a reducible oxide, whereas the other oxides are irreducible. Oxygen atoms in the pristine surfaces have a slight negative CLS with respect to the bulk references. The presence of oxygen vacancies is found to have a negligible effect on the O1s core level binding energy on neighboring oxygen atoms. The absence of shifts is connected to the fact that the valence electronic density is close to unaffected by the presence of vacancies in the case of the irreducible oxide. We speculate that the common assignment of positive shifts to oxygen vacancies could be related to different types of OH groups on the surfaces.

CRediT authorship contribution statement

Alvaro Posada-Borbón: Investigation, Writing - original draft. **Noemi Bosio:** Investigation, Writing - original draft. **Henrik Grönbeck:** Investigation, Writing - original draft, Supervision.

Declaration of Competing Interest

The authors have no conflict of interest.

Acknowledgement

Financial support from the Knut and Alice Wallenberg Foundation through the project "Atomistic design of catalysts" (No: KAW 2015.0058) and the Swedish Research Council (2016-05234) is gratefully acknowledged. The calculations have been performed at C3SE (Göteborg) and PDC (Stockholm) through a SNIC grant. The Competence Centre for Catalysis is hosted by Chalmers University of Technology and financially supported by the Swedish Energy Agency and the member companies AB Volvo, ECAPS AB, Johnson Matthey AB, Preem AB, Scania CV AB, and Umicore Denmark Aps.

References

[1] K. Siegbahn, Rev. Mod. Phys. 54 (3) (1982) 709.
[2] J.N. Andersen, D. Hennig, E. Lundgren, M. Methfessel, R. Nyholm, M. Scheffler, Phys. Rev. B 50 (1994) 17525.
[3] P. Kostelnik, N. Seriani, G. Kresse, A. Mikkelsen, E. Lundgren, V. Blum, T. Sikola, P. Varga, M. Schmid, Surf. Sci. 601 (2007) 1574.
[4] J. Gustafson, M. Borg, A. Mikkelsen, S. Gorovikov, E. Lundgren, J. Andersen, Phys. Rev. Lett. 91 (5) (2003) 056102.
[5] B. Johansson, N. Mårtensson, Phys. Rev. B 21 (1980) 4427.
[6] H. Grönbeck, S. Klacar, N.M. Martin, A. Hellman, E. Lundgren, J.N. Andersen, Phys. Rev. B 85 (2012) 115445.
[7] X. Zhang, J. Qin, Y. Xue, P. Yu, B. Zhang, L. Wang, R. Liu, Sci. Rep. 4 (2014) 4596.
[8] J. Fang, H. Fan, Y. Ma, Z. Wang, Q. Chang, Appl. Surf. Sci. 332 (2015) 47–54.
[9] J. Pilz, A. Perrotta, P. Christian, M. Tazreiter, R. Resel, G. Leising, T. Griesser, A. M. Coclite, J. Vac. Sci. Techn. A 36 (1) (2018) 01A109.
[10] J.C.C. Fan, J.B. Goodenough, J. Appl. Phys. 48 (8) (1977) 3524–3531.
[11] M.S. Frei, C. Mondelli, R. Garcia-Muelas, K.S. Kley, B. Puertolas, N. Lopez, O. Safonova V, J.A. Stewart, D.C. Ferre, J. Perez-Ramirez, Nat. Commun. 10 (2019) 3377.
[12] B. Lindberg, K. Hamrin, G. Johansson, U. Gelius, A. Fahlman, C. Nordling, K. Siegbahn, Phys. Scr. 1 (1970) 286.
[13] H. Gelius, Phys. Scr. 9 (1974) 133.
[14] P.S. Bagus, F. Illas, G. Pacchioni, F. Parmigiani, J. Elec. Spec. Rel. Phen. 100 (1999) 215.
[15] M. Weinert, R.E. Watson, Phys. Rev. B 51 (1995) 17168.
[16] I.A. Abrikosov, W. Olovsson, B. Johansson, Phys. Rev. Lett. 87 (2001) 176403.
[17] G. Kresse, J. Hafner, Phys. Rev. B 47 (1993) 558.
[18] G. Kresse, J. Hafner, Phys. Rev. B 49 (1993) 14251.
[19] G. Kresse, J. Furthmüller, Comput. Mater. Sci. 6 (1996) 15.
[20] G. Kresse, J. Furthmüller, Phys. Rev. B 54 (1996) 11169.
[21] P.E. Blöchl, Phys. Rev. B 50 (1994) 17953.
[22] G. Kresse, D. Joubert, Phys. Rev. B 59 (1999) 1758.
[23] J.P. Perdew, K. Burke, M. Ernzerhof, Phys. Rev. Lett. 77 (1996) 3865.
[24] S.L. Dudarev, G.A. Botton, S.Y. Savrasov, C.J. Humphreys, A.P. Sutton, Phys. Rev. B 57 (3) (1998) 1505–1509.
[25] P. Erhart, K. Albe, A. Klein, Phys. Rev. B 73 (20) (2006) 205203.
[26] M. Huang, S. Fabris, J. Phys. Chem. C 112 (2008) 8643–8648.
[27] H.J. Monkhorst, J.D. Pack, Phys. Rev. B 13 (1976) 5188.
[28] J.D. Pack, H.J. Monkhorst, Phys. Rev. B 16 (1977) 1748.
[29] E. Pehlke, M. Scheffler, Phys. Rev. Lett. 71 (1993) 2338.
[30] N. Mårtensson, A. Nilsson, J. Electron Spectrosc. Relat. Phenom. 75 (1995) 209.
[31] M. Van den Bossche, N.M. Martin, J. Gustafson, C. Hakanoglu, J. Weaver, E. Lundgren, H. Grönbeck, J. Chem. Phys. 141 (2014) 034706.
[32] F.A. Delesma, M. Van den Bossche, H. Grönbeck, P. Calaminici, A.M. Koster, L.G. M. Pettersson, ChemPhysChem 19 (2) (2018) 169–174.
[33] P. Broqvist, H. Grönbeck, I. Panas, Surf. Sci. 554 (2-3) (2004) 262–271.
[34] L.O. Paz-Borbon, A. Hellman, H. Grönbeck, J. Phys. Chem. C 116 (2012) 3545.
[35] C.J. Nelin, F. Uhl, V. Staemmler, P.S. Bagus, Y. Fujimori, M. Sterrer, H. Kuhlenbeck, H.-J. Freund, Phys. Chem. Chem. Phys. 16 (40) (2014) 21953–21956.
[36] Y.K. Gao, F. Traeger, O. Shekhah, H. Idriss, C. Woell, J. Colloid Interface Sci. 338 (1) (2009) 16–21.
[37] K. Kotsis, V. Staemmler, Phys. Chem. Chem. Phys. 16 (40) (2014) 21953–21956.
[38] R. Bader, Atoms in Molecules: A quantum theory, Oxford University Press, New York, 1990.
[39] W. Tang, E. Sanville, G. Henkelman, Journal of Physics: Condensed Matter 21 (2009) 084204.
[40] Y. Pan, N. Nillius, H.-J. Freund, J. Paier, C. Penschke, J. Sauer, Phys. Rev. Lett. 41 (1978) 1425.
[41] Z.K. Han, Y.Z. Yang, B. Zhu, M.V. Ganduglia-Pirovano, Y. Gao, Phys. Rev. Mater. 2 (2018) 035802.
[42] A. Posada-Borbón, H. Grönbeck, Phys. Chem. Chem. Phys. 21 (2019) 21667.
[43] A. Posada-Borbón, H. Grönbeck, Phys. Chem. Chem. Phys 22 (2020) 16193.
[44] D. Fernandez-Torre, J. Carrasco, M. Ganduglia-Pirovano, P. Perez, J. Chem. Phys. 141 (2014) 014703.